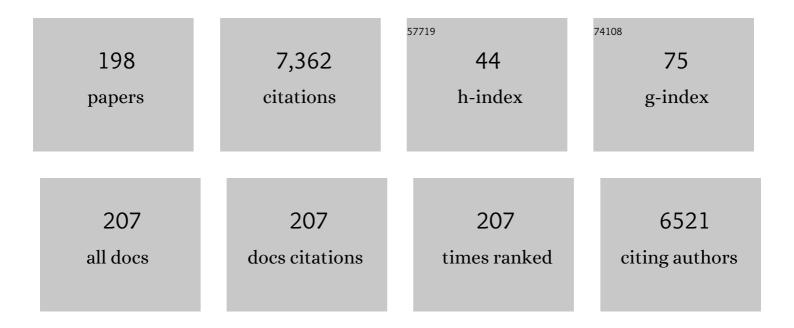
List of Publications by Year in descending order

Source: https://exaly.com/author-pdf/1183668/publications.pdf Version: 2024-02-01



#	Article	IF	CITATIONS
1	Processing of Generator-Produced 68Ga for Medical Application. Journal of Nuclear Medicine, 2007, 48, 1741-1748.	2.8	445
2	Correlation Between Dopamine D2 Receptors in the Ventral Striatum and Central Processing of Alcohol Cues and Craving. American Journal of Psychiatry, 2004, 161, 1783-1789.	4.0	341
3	Correlation of Alcohol Craving With Striatal Dopamine Synthesis Capacity and D2/3Receptor Availability: A Combined [18F]DOPA and [18F]DMFP PET Study in Detoxified Alcoholic Patients. American Journal of Psychiatry, 2005, 162, 1515-1520.	4.0	253
4	Association of Low Striatal Dopamine D ₂ Receptor Availability With Nicotine Dependence Similar to That Seen With Other Drugs of Abuse. American Journal of Psychiatry, 2008, 165, 507-514.	4.0	189
5	The Renaissance of the 68Ce/68Ca Radionuclide Generator Initiates New Developments in 68Ga Radiopharmaceutical Chemistry. Current Topics in Medicinal Chemistry, 2010, 10, 1633-1668.	1.0	169
6	High opiate receptor binding potential in the human lateral pain system. Neurolmage, 2006, 30, 692-699.	2.1	157
7	Generator-based PET radiopharmaceuticals for molecular imaging of tumours: on the way to THERANOSTICS. Dalton Transactions, 2011, 40, 6104.	1.6	148
8	Brain and Plasma Pharmacokinetics of Aripiprazole in Patients With Schizophrenia: An [¹⁸ F]Fallypride PET Study. American Journal of Psychiatry, 2008, 165, 988-995.	4.0	139
9	A Triazacyclononaneâ€Based Bifunctional Phosphinate Ligand for the Preparation of Multimeric ⁶⁸ Ga Tracers for Positron Emission Tomography. Chemistry - A European Journal, 2010, 16, 7174-7185.	1.7	138
10	Positron Emission Tomography in CNS Drug Discovery and Drug Monitoring. Journal of Medicinal Chemistry, 2014, 57, 9232-9258.	2.9	129
11	Preliminary data on biodistribution and dosimetry for therapy planning of somatostatin receptor positive tumours: comparison of 86Y-DOTATOC and 111In-DTPA-octreotide. European Journal of Nuclear Medicine and Molecular Imaging, 2001, 28, 1743-1750.	3.3	127
12	The Beginning and Development of the Theranostic Approach in Nuclear Medicine, as Exemplified by the Radionuclide Pair 86Y and 90Y. Pharmaceuticals, 2017, 10, 56.	1.7	114
13	Radioactive Labeling of Defined HPMA-Based Polymeric Structures Using [¹⁸ F]FETos for In Vivo Imaging by Positron Emission Tomography. Biomacromolecules, 2009, 10, 1697-1703.	2.6	99
14	Vascular Imaging of Solid Tumors in Rats with a Radioactive Arsenic-Labeled Antibody that Binds Exposed Phosphatidylserine. Clinical Cancer Research, 2008, 14, 1377-1385.	3.2	98
15	A 44Ti/44Sc radionuclide generator for potential application of 44Sc-based PET-radiopharmaceuticals. Radiochimica Acta, 2010, 98, .	0.5	98
16	The Striatal and Extrastriatal D2/D3 Receptor-Binding Profile of Clozapine in Patients with Schizophrenia. Neuropsychopharmacology, 2006, 31, 1027-1035.	2.8	96
17	Clinical Translation and First In-Human Use of [⁴⁴ Sc]Sc-PSMA-617 for PET Imaging of Metastasized Castrate-Resistant Prostate Cancer. Theranostics, 2017, 7, 4359-4369.	4.6	94
18	Validation of 68Ge/68Ga generator processing by chemical purification for routine clinical application of 68Ga-DOTATOC. Nuclear Medicine and Biology, 2008, 35, 721-724.	0.3	93

#	Article	IF	CITATIONS
19	Decreased Dopamine D2/D3-Receptor Binding in Temporal Lobe Epilepsy: An [18F]Fallypride PET Study. Epilepsia, 2006, 47, 1392-1396.	2.6	92
20	Biodistribution, pharmacokinetics, dosimetry of [68Ga]Ga-DOTA.SA.FAPi, and the head-to-head comparison with [18F]F-FDG PET/CT in patients with various cancers. European Journal of Nuclear Medicine and Molecular Imaging, 2021, 48, 1915-1931.	3.3	88
21	PET-pharmacokinetics of 18F-octreotide: A comparison with 67Ga-DFO and 86Y-DTPA-octreotide. Nuclear Medicine and Biology, 1997, 24, 275-286.	0.3	85
22	A theranostic approach of [68Ga]Ga-DOTA.SA.FAPi PET/CT-guided [177Lu]Lu-DOTA.SA.FAPi radionuclide therapy in an end-stage breast cancer patient: new frontier in targeted radionuclide therapy. European Journal of Nuclear Medicine and Molecular Imaging, 2021, 48, 942-944.	3.3	83
23	Radiochemical separation of no-carrier-added as produced via the process. Applied Radiation and Isotopes, 2000, 53, 421-425.	0.7	80
24	PET/CT imaging of osteoblastic bone metastases with 68Ga-bisphosphonates: first human study. European Journal of Nuclear Medicine and Molecular Imaging, 2010, 37, 834-834.	3.3	80
25	Bifunctional Gallium-68 Chelators: Past, Present, and Future. Seminars in Nuclear Medicine, 2016, 46, 373-394.	2.5	80
26	Structure and stability of hexadentate complexes of ligands based on AAZTA for efficient PET labelling with gallium-68. Chemical Communications, 2013, 49, 579-581.	2.2	75
27	Modifying the Body Distribution of HPMA-Based Copolymers by Molecular Weight and Aggregate Formation. Biomacromolecules, 2011, 12, 2841-2849.	2.6	72
28	Radiolabeling of DOTATOC with the long-lived positron emitter 44Sc. Applied Radiation and Isotopes, 2012, 70, 974-979.	0.7	69
29	Acute Blood Pressure Effects and Chronic Hypotensive Action of Calcimimetics in Uremic Rats. Journal of the American Society of Nephrology: JASN, 2006, 17, 655-662.	3.0	65
30	Asymmetry in dopamine D2/3 receptors of caudate nucleus is lost with age. NeuroImage, 2007, 34, 870-878.	2.1	65
31	Targeting fibroblast activation protein (FAP): next generation PET radiotracers using squaramide coupled bifunctional DOTA and DATA5m chelators. EJNMMI Radiopharmacy and Chemistry, 2020, 5, 19.	1.8	61
32	PEGylation of HPMA-based block copolymers enhances tumor accumulation in vivo : A quantitative study using radiolabeling and positron emission tomography. Journal of Controlled Release, 2013, 172, 77-85.	4.8	60
33	Ethanol-Based Post-processing of Generator-Derived ⁶⁸ Ga Toward Kit-Type Preparation of ⁶⁸ Ga-Radiopharmaceuticals. Journal of Nuclear Medicine, 2014, 55, 1023-1028.	2.8	56
34	Approaching â€~Kitâ€Type' Labelling with ⁶⁸ Ga: The DATA Chelators. ChemMedChem, 2015, 10, 1019-1026.	1.6	56
35	Inhibition of O6-Methylguanine-DNA Methyltransferase by Glucose-Conjugated Inhibitors: Comparison with Nonconjugated Inhibitors and Effect on Fotemustine and Temozolomide-Induced Cell Death. Journal of Pharmacology and Experimental Therapeutics, 2004, 311, 585-593.	1.3	54
36	First-In-Human Results on the Biodistribution, Pharmacokinetics, and Dosimetry of [177Lu]Lu-DOTA.SA.FAPi and [177Lu]Lu-DOTAGA.(SA.FAPi)2. Pharmaceuticals, 2021, 14, 1212.	1.7	52

#	Article	IF	CITATIONS
37	The dopamine D2 receptor ligand 18F-desmethoxyfallypride: an appropriate fluorinated PET tracer for the differential diagnosis of parkinsonism. European Journal of Nuclear Medicine and Molecular Imaging, 2004, 31, 1128-35.	3.3	51
38	High striatal occupancy of D2-like dopamine receptors by amisulpride in the brain of patients with schizophrenia. International Journal of Neuropsychopharmacology, 2004, 7, 421-430.	1.0	50
39	Gallium(III) complexes of NOTAâ€bis (phosphonate) conjugates as PET radiotracers for bone imaging. Contrast Media and Molecular Imaging, 2015, 10, 122-134.	0.4	50
40	NODAPA-OH and NODAPA-(NCS)n: Synthesis, 68Ga-radiolabelling and in vitro characterisation of novel versatile bifunctional chelators for molecular imaging. Bioorganic and Medicinal Chemistry Letters, 2008, 18, 5364-5367.	1.0	49
41	Net influx of plasma 6-[18F]fluoro-l-DOPA (FDOPA) to the ventral striatum correlates with prefrontal processing of affective stimuli. European Journal of Neuroscience, 2006, 24, 305-313.	1.2	48
42	Radiolanthanides in endoradiotherapy: an overview. Radiochimica Acta, 2007, 95, 303-311.	0.5	48
43	Electrochemical separation and purification of yttrium-86. Radiochimica Acta, 2002, 90, 225-228.	0.5	47
44	[18 F]Fluoroethylflumazenil: a novel tracer for PET imaging of human benzodiazepine receptors. European Journal of Nuclear Medicine and Molecular Imaging, 2001, 28, 1463-1470.	3.3	46
45	Novel Radiolabeled Bisphosphonates for PET Diagnosis and Endoradiotherapy of Bone Metastases. Pharmaceuticals, 2017, 10, 45.	1.7	44
46	The Use of the Macrocyclic Chelator DOTA in Radiochemical Separations. European Journal of Inorganic Chemistry, 2020, 2020, 36-56.	1.0	44
47	On the consensus nomenclature rules for radiopharmaceutical chemistry – Reconsideration of radiochemical conversion. Nuclear Medicine and Biology, 2021, 93, 19-21.	0.3	43
48	Synthesis and Preliminary <i>in Vivo</i> Evaluation of Well-Dispersed Biomimetic Nanocrystalline Apatites Labeled with Positron Emission Tomographic Imaging Agents. ACS Applied Materials & Interfaces, 2015, 7, 10623-10633.	4.0	42
49	DATATOC: a novel conjugate for kit-type 68Ga labelling of TOC at ambient temperature. EJNMMI Radiopharmacy and Chemistry, 2017, 1, 4.	1.8	41
50	72/74As-labeling of HPMA based polymers for long-term in vivo PET imaging. Bioorganic and Medicinal Chemistry Letters, 2010, 20, 5454-5458.	1.0	40
51	A no-carrier-added 72Se/72As radionuclide generator based on solid phase extraction. Radiochimica Acta, 2005, 93, .	0.5	39
52	Cross section data for the production of the positron emitting niobium isotope 90Nb via the 90Zr(p,) Tj ETQq0 0	0 rgBT /O	verlock 10 Tf

53	Efficient alkali iodide promoted 18F-fluoroethylations with 2-[18F]fluoroethyl tosylate and 1-bromo-2-[18F]fluoroethane. Tetrahedron Letters, 2003, 44, 9165-9167.	0.7	38
54	Synthesis and in vitro affinities of various MDL 100907 derivatives as potential 18F-radioligands for 5-HT2A receptor imaging with PET. Bioorganic and Medicinal Chemistry, 2009, 17, 2989-3002.	1.4	38

#	Article	IF	CITATIONS
55	In vivo comparison of DOTA based 68Ga-labelled bisphosphonates for bone imaging in non-tumour models. Nuclear Medicine and Biology, 2013, 40, 823-830.	0.3	38
56	New Frontiers in Cancer Imaging and Therapy Based on Radiolabeled Fibroblast Activation Protein Inhibitors: A Rational Review and Current Progress. Pharmaceuticals, 2021, 14, 1023.	1.7	38
57	Potential use of 68Ga-apo-transferrin as a PET imaging agent for detecting Staphylococcus aureus infection. Nuclear Medicine and Biology, 2011, 38, 393-398.	0.3	37
58	177Lu-labelled macrocyclic bisphosphonates for targeting bone metastasis in cancer treatment. EJNMMI Research, 2016, 6, 5.	1.1	36
59	Evaluation of bone-seeking novel radiotracer 68Ga-NO2AP-Bisphosphonate for the detection of skeletal metastases in carcinoma breast. European Journal of Nuclear Medicine and Molecular Imaging, 2017, 44, 41-49.	3.3	36
60	The applicability of SRTM in [18F]fallypride PET investigations: Impact of scan durations. Journal of Cerebral Blood Flow and Metabolism, 2011, 31, 1958-1966.	2.4	35
61	Comparison of different phosphorus-containing ligands complexing68Ga for PET-imaging of bone metabolism. Radiochimica Acta, 2011, 99, 43-51.	0.5	35
62	Synthesis and in vitro evaluation of (S)-2-([11C]methoxy)-4-[3-methyl-1-(2-piperidine-1-yl-phenyl)-butyl-carbamoyl]-benzoic acid ([11C]methoxy-repaglinide): a potential Î ² -cell imaging agent. Bioorganic and Medicinal Chemistry Letters, 2004, 14, 5205-5209.	1.0	34
63	Opiate-Induced Dopamine Release Is Modulated by Severity of Alcohol Dependence: An [18F]Fallypride Positron Emission Tomography Study. Biological Psychiatry, 2011, 70, 770-776.	0.7	34
64	A no-carrier-added 72Se/72As radionuclide generator based on distillation. Radiochimica Acta, 2004, 92, 245-249.	0.5	33
65	Total synthesis and evaluation of [18F]MHMZ. Bioorganic and Medicinal Chemistry Letters, 2008, 18, 1515-1519.	1.0	33
66	Dopamine D2/3 receptor occupancy by quetiapine in striatal and extrastriatal areas. International Journal of Neuropsychopharmacology, 2010, 13, 951-960.	1.0	33
67	Imaging of Protein Synthesis: In Vitro and In Vivo Evaluation of 44Sc-DOTA-Puromycin. Molecular Imaging and Biology, 2013, 15, 79-86.	1.3	33
68	A 140Nd/140Pr radionuclide generator based on physico-chemical transitions in 140Pr complexes after electron capture decay of 140Nd-DOTA. Radiochimica Acta, 2007, 95, 319-327.	0.5	31
69	HPMA Based Amphiphilic Copolymers Mediate Central Nervous Effects of Domperidone. Macromolecular Rapid Communications, 2011, 32, 712-717.	2.0	31
70	Novel Fibroblast Activation Protein Inhibitor-Based Targeted Theranostics for Radioiodine-Refractory Differentiated Thyroid Cancer Patients: A Pilot Study. Thyroid, 2021, , .	2.4	31
71	HPMA-LMA Copolymer Drug Carriers in Oncology: An in Vivo PET Study to Assess the Tumor Line-Specific Polymer Uptake and Body Distribution. Biomacromolecules, 2013, 14, 3091-3101.	2.6	30
72	From Bench to Bedside—The Bad Berka Experience With First-in-Human Studies. Seminars in Nuclear Medicine, 2019, 49, 422-437.	2.5	30

#	Article	IF	CITATIONS
73	<i>closo</i> -Borane Conjugated Regulatory Peptides Retain High Biological Affinity: Synthesis of <i>closo</i> -Borane Conjugated Tyr ³ -Octreotate Derivatives for BNCT. Bioconjugate Chemistry, 2008, 19, 1796-1802.	1.8	29
74	Radiolabelling and preliminary evaluation of 68Ga-tetrapyrrole derivatives as potential tracers for PET. Nuclear Medicine and Biology, 2013, 40, 280-288.	0.3	29
75	Preliminary results of biodistribution and dosimetric analysis of [68Ga]Ga-DOTAZOL: a new zoledronate-based bisphosphonate for PET/CT diagnosis of bone diseases. Annals of Nuclear Medicine, 2019, 33, 404-413.	1.2	29
76	Thermochromatographic separation of no-carrier-added 186Re or 188Re from tungsten targets relevant to nuclear medical applications. Radiochimica Acta, 2000, 88, 163-168.	0.5	28
77	AAZTA5/AAZTA5-TOC: synthesis and radiochemical evaluation with 68Ga, 44Sc and 177Lu. EJNMMI Radiopharmacy and Chemistry, 2019, 4, 18.	1.8	28
78	Synthesis of a Tyr3-octreotate conjugated closo-carborane [HC2B10H10]: a potential compound for boron neutron capture therapy. Tetrahedron Letters, 2003, 44, 9143-9145.	0.7	27
79	In vitro affinities of various halogenated benzamide derivatives as potential radioligands for non-invasive quantification of D2-like dopamine receptors. Bioorganic and Medicinal Chemistry, 2007, 15, 6819-6829.	1.4	27
80	Separation and purification of no-carrier-added arsenic from bulk amounts of germanium for use in radiopharmaceutical labelling. Radiochimica Acta, 2010, 98, 807-812.	0.5	27
81	Synthesis of131I-Labeled Glucose-Conjugated Inhibitors ofO6-Methylguanine-DNA Methyltransferase (MGMT) and Comparison with Nonconjugated Inhibitors as Potential Tools for in Vivo MGMT Imaging. Journal of Medicinal Chemistry, 2006, 49, 263-272.	2.9	26
82	Activation of P-glycoprotein (Pgp)-mediated drug efflux by extracellular acidosis: in vivo imaging with 68Ga-labelled PET tracer. European Journal of Nuclear Medicine and Molecular Imaging, 2010, 37, 1935-1942.	3.3	26
83	Preliminary in vivo and ex vivo evaluation of the 5-HT2A imaging probe [18F]MH.MZ. Nuclear Medicine and Biology, 2009, 36, 447-454.	0.3	25
84	⁹⁰ Nb – aÂpotential PET nuclide: production and labeling of monoclonal antibodies. Radiochimica Acta, 2012, 100, 857-864.	0.5	25
85	Vulnerability to psychotogenic effects of ketamine is associated with elevated D2/3-receptor availability. International Journal of Neuropsychopharmacology, 2013, 16, 745-754.	1.0	25
86	Equilibrium, Kinetic and Structural Properties of Gallium(III) and Some Divalent Metal Complexes Formed with the New DATA ^m and DATA ^{5m} Ligands. Chemistry - A European Journal, 2017, 23, 10358-10371.	1.7	25
87	Synthesis of 2-amino-6-(2-[18F]fluoro-pyridine-4-ylmethoxy)-9-(octyl-β-d-glucosyl)-purine: a novel radioligand for positron emission tomography studies of the O6-methylguanine-DNA methyltransferase (MGMT) status of tumour tissue. Tetrahedron Letters, 2002, 43, 6301-6304.	0.7	24
88	Limiting transport properties of lanthanide and actinide ions in pure water. Radiochimica Acta, 2003, 91, 473-478.	0.5	24
89	Improved radiolabeling of DOTATOC with trivalent radiometals for clinical application by addition of ethanol. EJNMMI Radiopharmacy and Chemistry, 2017, 1, 6.	1.8	24
90	Prediction of Normal Organ Absorbed Doses for [177Lu]Lu-PSMA-617 Using [44Sc]Sc-PSMA-617 Pharmacokinetics in Patients With Metastatic Castration Resistant Prostate Carcinoma. Clinical Nuclear Medicine, 2018, 43, 486-491.	0.7	24

#	Article	IF	CITATIONS
91	Evaluation of the inverse electron demand Diels-Alder reaction in rats using a scandium-44-labelled tetrazine for pretargeted PET imaging. EJNMMI Research, 2019, 9, 49.	1.1	24
92	Production of positron-emitting 110mIn via the process. Applied Radiation and Isotopes, 1997, 48, 19-26.	0.7	23
93	18F-Labeling and evaluation of novel MDL 100907 derivatives as potential 5-HT2A antagonists for molecular imaging. Nuclear Medicine and Biology, 2010, 37, 487-495.	0.3	23
94	A prospective intra-individual comparison of [68Ga]Ga-PSMA-11 PET/CT, [68Ga]Ga-NODAGAZOL PET/CT, and [99mTc]Tc-MDP bone scintigraphy for radionuclide imaging of prostate cancer skeletal metastases. European Journal of Nuclear Medicine and Molecular Imaging, 2021, 48, 134-142.	3.3	23
95	Image quality analysis of 44Sc on two preclinical PET scanners: a comparison to 68Ga. EJNMMI Physics, 2020, 7, 16.	1.3	23
96	Limiting transport properties and hydration numbers of actinyl ions in pure water. Radiochimica Acta, 2004, 92, .	0.5	22
97	Application of tris-allyl-DOTA in the preparation of DOTA–peptide conjugates. Tetrahedron Letters, 2006, 47, 5985-5988.	0.7	22
98	[44Sc]Sc-PSMA-617 Biodistribution and Dosimetry in Patients With Metastatic Castration-Resistant Prostate Carcinoma. Clinical Nuclear Medicine, 2018, 43, 323-330.	0.7	22
99	[68Ga]Ga-DO2A-(OBu-l-tyr)2: Synthesis, 68Ga-radiolabeling and in vitro studies of a novel 68Ga-DO2A-tyrosine conjugate as potential tumor tracer for PET. Bioorganic and Medicinal Chemistry Letters, 2009, 19, 3498-3501.	1.0	21
100	Surrogate markers for cerebral blood flow correlate with [¹⁸ F]â€fallypride binding potential at dopamine D _{2/3} receptors in human striatum. Synapse, 2013, 67, 199-203.	0.6	21
101	Cation exchange-based post-processing of 68Ga-eluate: A comparison of three solvent systems for labelling of DOTATOC, NO2APBP and DATAm. Applied Radiation and Isotopes, 2015, 98, 54-59.	0.7	21
102	Structure–Function Evaluation of Imidazopyridine Derivatives Selective for δ-Subunit-Containing γ-Aminobutyric Acid Type A (GABAA) Receptors. Journal of Medicinal Chemistry, 2018, 61, 1951-1968.	2.9	21
103	Improved Efficacy of Synthesizing *M ^{III} -Labeled DOTA Complexes in Binary Mixtures of Water and Organic Solvents. A Combined Radio- and Physicochemical Study. Inorganic Chemistry, 2018, 57, 6107-6117.	1.9	21
104	Evaluation of Safety and Dosimetry of ¹⁷⁷ Lu-DOTA-ZOL for Therapy of Bone Metastases. Journal of Nuclear Medicine, 2021, 62, 1126-1132.	2.8	21
105	<i>In vivo</i> Evaluation of [²²⁵ Ac]Ac-DOTA ^{ZOL} for α-Therapy of Bone Metastases. Current Radiopharmaceuticals, 2018, 11, 223-230.	0.3	21
106	Orthogonal Click Conjugation to the Liposomal Surface Reveals the Stability of the Lipid Anchorage as Crucial for Targeting. Chemistry - A European Journal, 2016, 22, 11578-11582.	1.7	20
107	Comparison of Linear and Hyperbranched Polyether Lipids for Liposome Shielding by ¹⁸ F-Radiolabeling and Positron Emission Tomography. Biomacromolecules, 2018, 19, 2506-2516.	2.6	20
108	Instant kit preparation of 68Ga-radiopharmaceuticals via the hybrid chelator DATA: clinical translation of [68Ga]Ga-DATA-TOC. EJNMMI Research, 2019, 9, 48.	1.1	20

#	Article	IF	CITATIONS
109	Synthesis and labeling of a squaric acid containing PSMA-inhibitor coupled to AAZTA5 for versatile labeling with 44Sc, 64Cu, 68Ga and 177Lu. Applied Radiation and Isotopes, 2020, 156, 108867.	0.7	20
110	Biodistribution and post-therapy dosimetric analysis of [177Lu]Lu-DOTAZOL in patients with osteoblastic metastases: first results. EJNMMI Research, 2019, 9, 102.	1.1	20
111	Radiosynthesis of 1-(4-(2-[18F]fluoroethoxy)benzenesulfonyl)-3-butyl urea: a potentialβ-cell imaging agent. Journal of Labelled Compounds and Radiopharmaceuticals, 2002, 45, 763-774.	0.5	19
112	A convenient chemo-enzymatic synthesis and 18F-labelling of both enantiomers of trans-1-toluenesulfonyloxymethyl-2-fluoromethyl-cyclopropane. Organic and Biomolecular Chemistry, 2008, 6, 4567.	1.5	19
113	Efficient post-processing of aqueous generator eluates facilitates 68Ga-labelling under anhydrous conditions. Radiochimica Acta, 2010, 98, .	0.5	19
114	A methodical ⁶⁸ Gaâ€labelling study of DO2Aâ€(butyl― <scp>l</scp> â€tyrosine) ₂ with cationâ€exchanger postâ€processed ⁶⁸ Ga: practical aspects of radiolabelling. Contrast Media and Molecular Imaging, 2011, 6, 492-498.		19
115	Fate of Linear and Branched Polyether-Lipids In Vivo in Comparison to Their Liposomal Formulations by ¹⁸ F-Radiolabeling and Positron Emission Tomography. Biomacromolecules, 2015, 16, 842-851.	2.6	19
116	Evaluation of a novel monoclonal antibody against tumor-associated MUC1 for diagnosis and prognosis of breast cancer. International Journal of Medical Sciences, 2019, 16, 1188-1198.	1.1	19
117	68Ga, 44Sc and 177Lu-labeled AAZTA5-PSMA-617: synthesis, radiolabeling, stability and cell binding compared to DOTA-PSMA-617 analogues. EJNMMI Radiopharmacy and Chemistry, 2020, 5, 28.	1.8	19
118	Ratio of dopamine synthesis capacity to D2 receptor availability in ventral striatum correlates with central processing of affective stimuli. European Journal of Nuclear Medicine and Molecular Imaging, 2008, 35, 1147-1158.	3.3	18
119	Development of a [¹⁷⁷ Lu]BPAMD Labeling Kit and an Automated Synthesis Module for Routine Bone Targeted Endoradiotherapy. Cancer Biotherapy and Radiopharmaceuticals, 2015, 30, 94-99.	0.7	18
120	A DOTA based bisphosphonate with an albumin binding moiety for delayed body clearance for bone targeting. Nuclear Medicine and Biology, 2016, 43, 670-678.	0.3	18
121	Radiochemical separation of no-carrier-added radioniobium from zirconiu targets for application of 90Nb-labelled compounds. Radiochimica Acta, 2002, 90, 411-415.	0.5	17
122	Rapid radiosynthesis of [¹¹ C] and [¹⁴ C]azelaic, suberic, and sebacic acids for <i>in vivo</i> mechanistic studies of systemic acquired resistance in plants. Journal of Labelled Compounds and Radiopharmaceuticals, 2012, 55, 39-43.	0.5	17
123	Desferrioxamine as an appropriate chelator for 90Nb: Comparison of its complexation properties for M-Df-Octreotide (M=Nb, Fe, Ga, Zr). Nuclear Medicine and Biology, 2014, 41, 721-727.	0.3	17
124	Gallium-68 and scandium-44 labelled radiotracers based on curcumin structure linked to bifunctional chelators: Synthesis and characterization of potential PET radiotracers. Journal of Inorganic Biochemistry, 2020, 204, 110954.	1.5	17
125	[⁶⁸ Ga]Ga-THP-Pam: A Bisphosphonate PET Tracer with Facile Radiolabeling and Broad Calcium Mineral Affinity. Bioconjugate Chemistry, 2021, 32, 1276-1289.	1.8	17
126	Squaric Acid-Based Radiopharmaceuticals for Tumor Imaging and Therapy. Bioconjugate Chemistry, 2021, 32, 1223-1231.	1.8	17

#	Article	IF	CITATIONS
127	Synthesis and evaluation of 5,7-dichloro-4-(3-{4-[4-(2-[18F]fluoroethyl)-piperazin-1-yl]-phenyl}-ureido)-1,2,3,4-tetrahydroquinoline-2-carboxylic acid as a potential NMDA ligand to study glutamatergic neurotransmission in vivo. Journal of Labelled Compounds and Radiopharmaceuticals, 2003, 46, 645-659.	² 0.5	16
128	Exâ€vivo and inâ€vivo Evaluation of [¹⁸ F]PR04.MZ in Rodents: A Selective Dopamine Transporter Imaging Agent. ChemMedChem, 2009, 4, 1480-1487.	1.6	16
129	[68Ga]Ga-DATA5m.SA.FAPi PET/CT: Specific Tracer-uptake in Focal Nodular Hyperplasia and potential Role in Liver Tumor Imaging. Nuklearmedizin - NuclearMedicine, 2020, 59, 387-389.	0.3	16
130	Selective binding to monoamine oxidase A: In vitro and in vivo evaluation of 18F-labeled Î ² -carboline derivatives. Bioorganic and Medicinal Chemistry, 2015, 23, 612-623.	1.4	15
131	Novel bifunctional DATA chelator for quick access to site-directed PET ⁶⁸ Ga-radiotracers: preclinical proof-of-principle with [Tyr ³]octreotide. Dalton Transactions, 2017, 46, 14584-14590.	1.6	15
132	Predicting the in vivo release from a liposomal formulation by IVIVC and non-invasive positron emission tomography imaging. European Journal of Pharmaceutical Sciences, 2010, 41, 71-77.	1.9	14
133	Optimization of Labeling PSMA ^{HBED} with Ethanol-Postprocessed ⁶⁸ Ga and Its Quality Control Systems. Journal of Nuclear Medicine, 2017, 58, 432-437.	2.8	14
134	Measurement of the laser resonance ionization efficiency for lutetium. Radiochimica Acta, 2019, 107, 653-661.	0.5	14
135	Evaluation of [68Ga]Ga-DATA-TOC for imaging of neuroendocrine tumours: comparison with [68Ga]Ga-DOTA-NOC PET/CT. European Journal of Nuclear Medicine and Molecular Imaging, 2020, 47, 860-869.	3.3	14
136	First-in-Human Experience With 177Lu-DOTAGA.(SA.FAPi)2 Therapy in an Uncommon Case of Aggressive Medullary Thyroid Carcinoma Clinically Mimicking as Anaplastic Thyroid Cancer. Clinical Nuclear Medicine, 2022, 47, e444-e445.	0.7	14
137	Efficient microwave-assisted direct radiosynthesis of [18F]PRO4.MZ and [18F]LBT999: Selective dopamine transporter ligands for quantitative molecular imaging by means of PET. Bioorganic and Medicinal Chemistry, 2009, 17, 7630-7634.	1.4	13
138	Evaluation of P-glycoprotein (abcb1a/b) modulation of [18F]fallypride in MicroPET imaging studies. Neuropharmacology, 2014, 84, 152-158.	2.0	13
139	Fibroblast activation protein inhibitor (FAPi) positive tumour fraction on PET/CT correlates with Ki-67 in liver metastases of neuroendocrine tumours. Nuklearmedizin - NuclearMedicine, 2021, 60, 344-354.	0.3	13
140	[177Lu]Lu-DOTA-ZOL bone pain palliation in patients with skeletal metastases from various cancers: efficacy and safety results. EJNMMI Research, 2020, 10, 130.	1.1	13
141	Radiosynthesis of		

#	Article	IF	CITATIONS
145	Assessing p-Glycoprotein (Pgp) Activity In Vivo Utilizing 68Ga–Schiff Base Complexes. Molecular Imaging and Biology, 2011, 13, 985-994.	1.3	11
146	Promoting Experimental Problem-solving Ability in Sixth-grade Students Through Problem-oriented Teaching of Ecology: Findings of an intervention study in a complex domain. International Journal of Science Education, 2015, 37, 577-598.	1.0	11
147	Behavior of Actinium, Alkaline, and Rare Earth Elements in Sr-Resin/Mineral Acid Systems. Solvent Extraction and Ion Exchange, 2015, 33, 496-509.	0.8	11
148	Pharmacokinetic evaluation of [18F]PR04.MZ for PET/CT imaging and quantification of dopamine transporters in the human brain. European Journal of Nuclear Medicine and Molecular Imaging, 2020, 47, 1927-1937.	3.3	11
149	Targeting of Immune Cells with Trimannosylated Liposomes. Advanced Therapeutics, 2020, 3, 1900185.	1.6	11
150	Synthesis, Labeling and Preclinical Evaluation of a Squaric Acid Containing PSMA Inhibitor Labeled with ⁶⁸ Ga: A Comparison with PSMAâ€1 and PSMAâ€617. ChemMedChem, 2020, 15, 695-704.	1.6	11
151	Quantitative online isolation of 68Ge from 68Ge/68Ga generator eluates for purification and immediate quality control of breakthrough. Applied Radiation and Isotopes, 2013, 82, 45-48.	0.7	10
152	Synthesis and preliminary evaluation of (R,R)(S,S) 5-(2-(2-[4-(2-[18F]fluoroethoxy)phenyl]-1-methylethylamino)-1-hydroxyethyl)-benzene-1,3-diol ([18F]FEFE) for the in vivo visualisation and quantification of the l²2-adrenergic receptor status in lung. Bioorganic and Medicinal Chemistry Letters, 2003, 13, 2687-2692.	1.0	9
153	Automated synthesis and purification of [¹⁸ F]fluoroâ€{ <i>diâ€deutero</i>]methyl tosylate. Journal of Labelled Compounds and Radiopharmaceuticals, 2013, 56, 360-363.	0.5	9
154	Imaging Nigrostriatal Dopaminergic Deficit in Holmes Tremor with 18F-PR04.MZ-PET/CT. Clinical Nuclear Medicine, 2015, 40, 740-741.	0.7	9
155	Labeling of DOTA-conjugated HPMA-based polymers with trivalent metallic radionuclides for molecular imaging. EJNMMI Research, 2018, 8, 16.	1.1	9
156	Comparison Study of Two Differently Clicked 18F-Folates—Lipophilicity Plays a Key Role. Pharmaceuticals, 2018, 11, 30.	1.7	9
157	PET Imaging of the Impact of Extracellular pH and MAP Kinases on the p-Glycoprotein (Pgp) Activity. Advances in Experimental Medicine and Biology, 2013, 765, 279-286.	0.8	9
158	An approach to the evaluation of the activity of the DNA repair enzyme O6-methylguanine-DNA-methyl-transferase in tumor tissue in vivo: syntheses of 6-benzyloxy-9-(2-[18F]fluoroethyl)-9H-purin-2-yl-amine and 6-benzyloxy-7-(2-[18F]fluoroethyl)-7H-purin-2-yl-amine. Applied Radiation and Isotopes, 2002, 56, 511-517.	0.7	8
159	Synthesis of novel WAY 100635 derivatives containing a norbornene group and radiofluorination of [18F]AH1.MZ as a serotonin 5-HT1Areceptor antagonist for molecular imaging. Journal of Labelled Compounds and Radiopharmaceuticals, 2009, 52, 201-207.	0.5	8
160	Synthesis and radiosynthesis of N5-[18F]fluoroethyl-Pirenzepine and its metabolite N5-[18F]fluoroethyl-LS 75. Journal of Labelled Compounds and Radiopharmaceuticals, 2009, 52, n/a-n/a.	0.5	8
161	Twoâ€step radiosynthesis of [¹⁸ F]FEâ€ <i>β</i> IT and [¹⁸ F]PR04.MZ. Journal of Labelled Compounds and Radiopharmaceuticals, 2013, 56, 356-359.	0.5	7
162	Direct flow separation strategy, to isolate no-carrier-added ⁹⁰ Nb from irradiated Mo or Zr targets. Radiochimica Acta, 2016, 104, 625-634.	0.5	7

#	Article	IF	CITATIONS
163	Long-term biodistribution study of HPMA- ran -LMA copolymers in vivo by means of 131 I-labeling. Nuclear Medicine and Biology, 2018, 58, 59-66.	0.3	7
164	AAZTA5-squaramide ester competing with DOTA-, DTPA- and CHX-A″-DTPA-analogues: Promising tool for 177Lu-labeling of monoclonal antibodies under mild conditions. Nuclear Medicine and Biology, 2021, 96-97, 80-93.	0.3	7
165	Complex formation of Tb3+ with glycolate, D-gluconate and α-isosaccharinate in neutral aqueous perchlorate solutions. Radiochimica Acta, 2003, 91, 599-602.	0.5	6
166	[11C]PR04.MZ, a promising DAT ligand for low concentration imaging: Synthesis, efficient 11C-O-methylation and initial small animal PET studies. Bioorganic and Medicinal Chemistry Letters, 2009, 19, 4343-4345.	1.0	6
167	A concise synthesis procedure to furnish multi-gram amounts of hexadentate, bivalent DO2A-based chelators. RSC Advances, 2012, 2, 7156.	1.7	6
168	Direct radiofluorination of [¹⁸ F]MH.MZ for 5â€HT _{2A} receptor molecular imaging with PET. Journal of Labelled Compounds and Radiopharmaceuticals, 2012, 55, 354-358.	0.5	6
169	Characterisation of [11C]PRO4.MZ in Papio anubis baboon: A selective high-affinity radioligand for quantitative imaging of the dopamine transporter. Bioorganic and Medicinal Chemistry Letters, 2012, 22, 679-682.	1.0	6
170	Characterization of the serotonin 2A receptor selective PET tracer (R)-[18F]MH.MZ in the human brain. European Journal of Nuclear Medicine and Molecular Imaging, 2020, 47, 355-365.	3.3	6
171	Development and in vitro evaluation of new bifunctional 89Zr-chelators based on the 6-amino-1,4-diazepane scaffold for immuno-PET applications. Nuclear Medicine and Biology, 2021, 102-103, 12-23.	0.3	6
172	Effect of the versatile bifunctional chelator AAZTA5 on the radiometal labelling properties and the in vitro performance of a gastrin releasing peptide receptor antagonist. EJNMMI Radiopharmacy and Chemistry, 2020, 5, 29.	1.8	6
173	Research Letter: Structural Combination of Established 5â€HT _{2A} Receptor Ligands: New Aspects of the Binding Mode. Chemical Biology and Drug Design, 2010, 76, 361-366.	1.5	5
174	P-Glycoprotein Influence on the Brain Uptake of a 5-HT _{2A} Ligand: [¹⁸ F]MH.MZ. Neuropsychobiology, 2011, 63, 183-190.	0.9	5
175	Impact of prompt gamma emission of 44Sc on quantification in preclinical and clinical PET systems. Applied Radiation and Isotopes, 2021, 170, 109599.	0.7	5
176	Mild and efficient ⁶⁴ Cu labeling of perhydro-1, 4-diazepine derivatives for potential use with large peptides, proteins and antibodies. Radiochimica Acta, 2020, 108, 555-563.	0.5	5
177	Hybrid Chelator-Based PSMA Radiopharmaceuticals: Translational Approach. Molecules, 2021, 26, 6332.	1.7	5
178	Ternary Complex Formation of Lanthanides and Radiolanthanides with Phosphate and Serum Proteins. Radiochimica Acta, 1999, 84, 201-204.	0.5	4
179	Synthesis of a technetium-99m labelledL-tyrosine derivative with thefac-99mTc(l)(CO)3-core using a simple kit-procedure. Journal of Labelled Compounds and Radiopharmaceuticals, 2004, 47, 477-483.	0.5	4
180	Preliminary assessment of the imaging capability of the YAP–(S)PET small animal scanner in neuroscience. Nuclear Instruments and Methods in Physics Research, Section A: Accelerators, Spectrometers, Detectors and Associated Equipment, 2006, 569, 488-491.	0.7	4

#	Article	IF	CITATIONS
181	Studies towards the development of lipophilic bifunctional N ₃ S ₃ chelators for ⁶⁸ Ga. Radiochimica Acta, 2010, 98, 519-523.	0.5	4
182	68Ge content quality control of 68Ge/68Ga-generator eluates and 68Ga radiopharmaceuticals – A protocol for determining the 68Ge content using thin-layer chromatography. Applied Radiation and Isotopes, 2014, 91, 92-96.	0.7	4
183	NMR Hyperpolarization of Established PET Tracers. ChemistrySelect, 2018, 3, 5176-5184.	0.7	4
184	[177Lu]Lu-DOTA-zoledronate therapy – first application in a patient with primary osseous metastatic bronchial carcinoma. Nuklearmedizin - NuclearMedicine, 2020, 59, 281-283.	0.3	4
185	Ternary Complex Formation between Yttrium, Phosphate and Serum Proteins. Radiochimica Acta, 1998, 81, 171-178.	0.5	3
186	A device for on-line electromigration measurements of radioelements in free electrolytes. Radiochimica Acta, 2000, 88, 399-404.	0.5	3
187	Electroosmotic effects in the determination of ion mobilities of carrier-free radionuclides in free aqueous electrolyte solutions. Radiochimica Acta, 2001, 89, 537-542.	0.5	3
188	Synthesis and evaluation of tritium labelled 10-methylgalanthamine iodide: a novel compound to examine the mechanism of interaction of galanthamine derivatives with the nicotinic acetylcholine receptors. Journal of Labelled Compounds and Radiopharmaceuticals, 2003, 46, 1117-1125.	0.5	3
189	The DAT Ligand [¹⁸ F]PR17.MZ Mirrors the inâ€vivo Pharmacokinetic Profile of [¹¹ C]Cocaine with Significantly Improved Monoamine Transporter Selectivity. ChemMedChem, 2010, 5, 1686-1688.	1.6	3
190	Reply: Impurity in 68Ca-Peptide Preparation Using Processed Generator Eluate. Journal of Nuclear Medicine, 2010, 51, 495.2-496.	2.8	1
191	Macromol. Rapid Commun. 9–10/2011. Macromolecular Rapid Communications, 2011, 32, .	2.0	1
192	Copper-catalyzed click reactions: quantification of retained copper using ⁶⁴ Cu-spiked Cu(I), exemplified for CuAAC reactions on liposomes. Radiochimica Acta, 2019, 107, 547-554.	0.5	1
193	Fibroblast Activation Protein (FAP) targeting homodimeric FAP inhibitor radiotheranostics: a step to improve tumor uptake and retention time American Journal of Nuclear Medicine and Molecular Imaging, 2021, 11, 476-491.	1.0	1
194	Squaric Acid Bisphposphonates for Theranostics of Bone Metastasis – the Easy DOTA-Zoledronate. Frontiers in Nuclear Medicine, 2022, 2, .	0.7	1
195	Automated GMP production of [11C]PR04.MZ via the captive solvent method and PET studies in non-human primates: A promising tracer for extrastriatal DAT imaging. NeuroImage, 2010, 52, S117.	2.1	Ο
196	Equilibrium in [18F]fallypride PET. NeuroImage, 2010, 52, S160.	2.1	0
197	Nuclear transformations and radioactive emissions: Part l—primary transformation pathways of unstable nuclei. ChemTexts, 2018, 4, 1.	1.0	0
198	Nuclear transformations and radioactive emissions: Part Il—secondary transitions and post-effects. ChemTexts, 2018, 4, 1.	1.0	0